

FIGURE 2.1 Example of a motor transmitting power, through shaft AB , to a power tool.

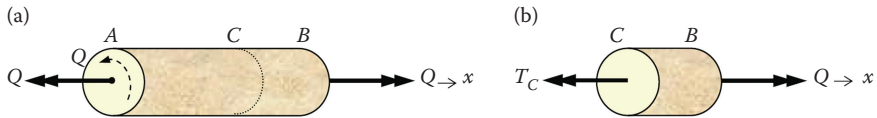


FIGURE 2.3 Representation of a concentrated torque Q at the center point in a circular shaft.

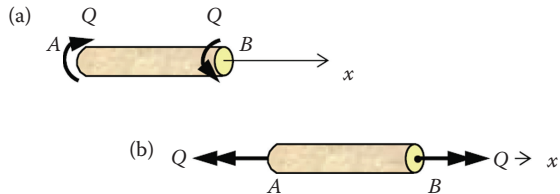


FIGURE 2.2 Representation of a three-dimensional torque Q by a double-headed arrow. Interpretation is made by the right-hand rule.

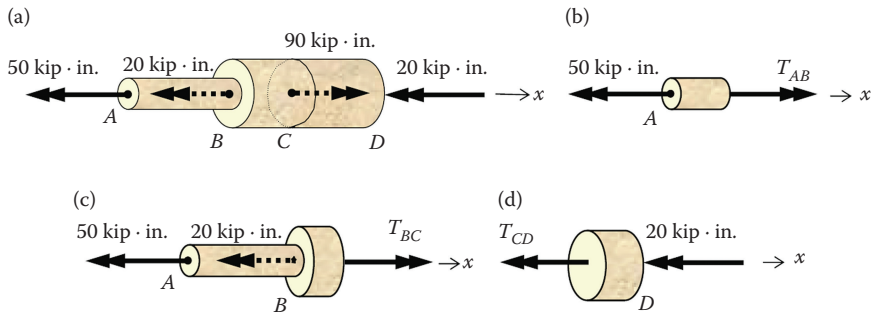


FIGURE 2.4 Shaft subjected to concentrated torques at a number of positions along its length, and determination of internal torques in segments AB, BC, and CD using equilibrium.

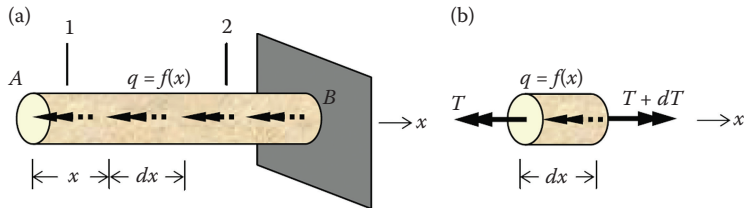


FIGURE 2.6 Example of a variably distributed torque $q = f(x)$ over the length of shaft AB and determination, using equilibrium, of internally distributed torque at any position in the shaft.

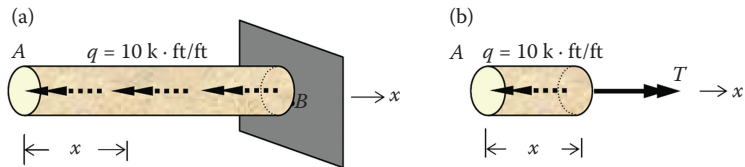


FIGURE 2.5 Example of a constantly distributed torque $q = 10 \text{ k} \cdot \text{ft/ft}$ over the entire length of the shaft AB and determination, by equilibrium, of internally distributed torque at any position a distance x from end A .

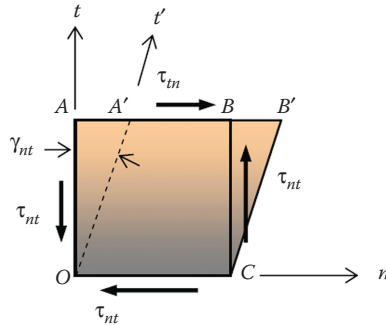


FIGURE 2.7 Definition of shearing strain γ_{nt} as being approximately equal to the tangent of the shearing angle γ_{nt} .

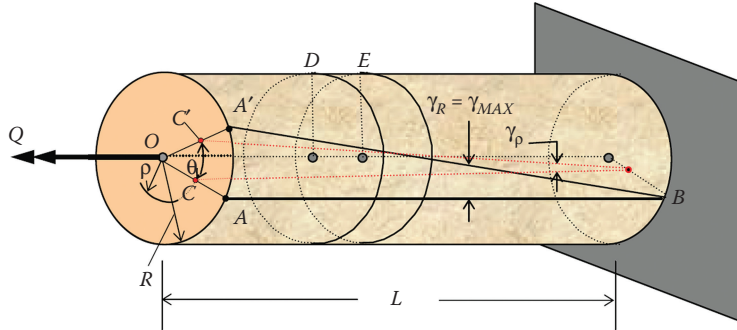


FIGURE 2.8 Shaft showing distortion under the influence of a torque Q and the definition of the angle of twist θ .

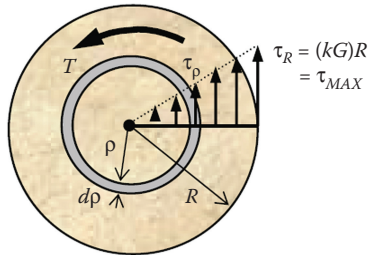


FIGURE 2.9 Circular cross section of a circular shaft showing the stress distribution due to a torque T .

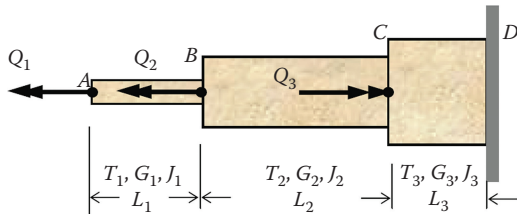


FIGURE 2.10 Shaft consisting of three component parts, each having its own properties T , G , and J , showing that the total angle of twist is the sum of three angles of twist.

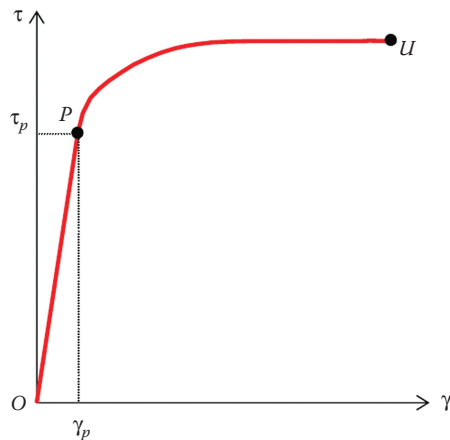


FIGURE 2.11 Shearing stress–strain diagram for a given ductile material, defining the properties: modulus of rigidity G and the modulus of rupture τ_U .

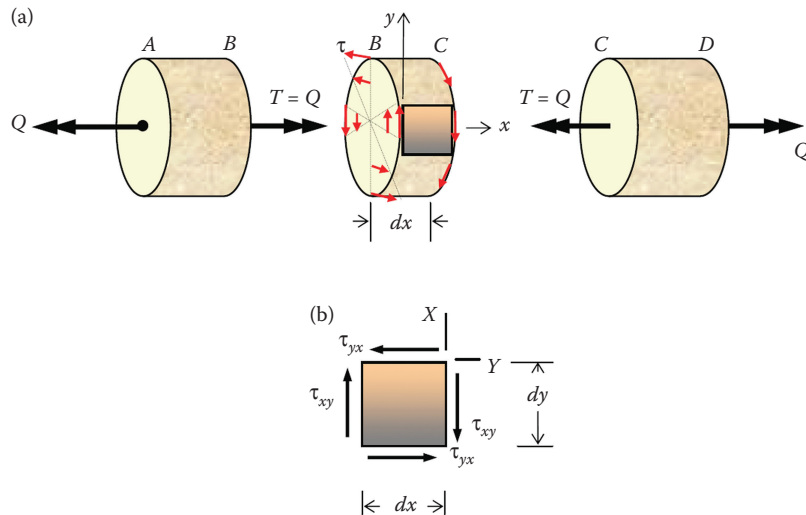


FIGURE 2.12 Diagram showing the state of pure shear in a shaft subjected to a torque Q .

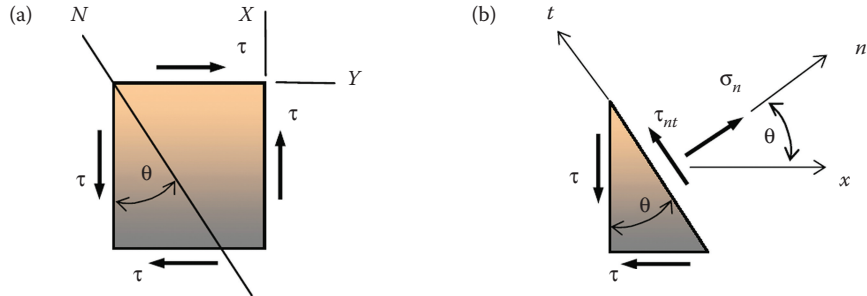


FIGURE 2.13 (a) The state of pure shear and (b) determination of normal and shearing stresses on inclined planes.

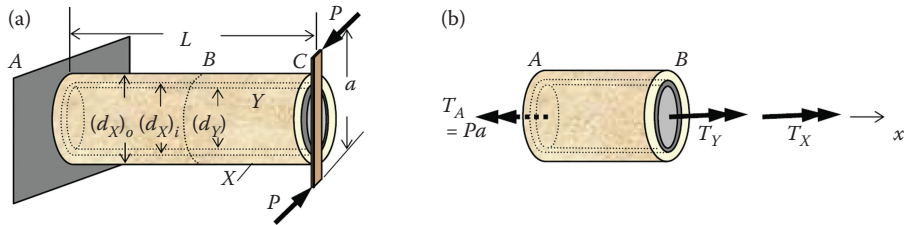


FIGURE 2.14 (a) A two-material shaft subjected to a torque Pa and (b) the free-body diagram of segment AB .

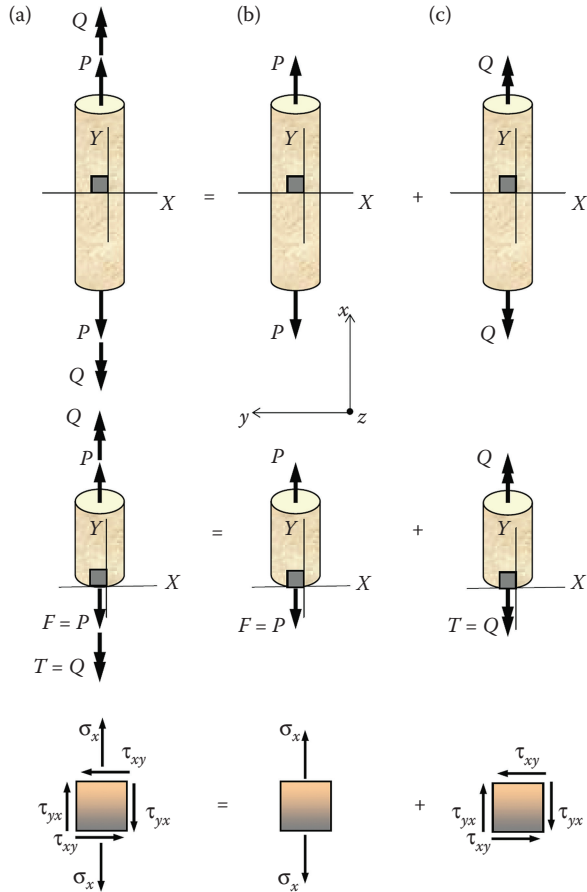


FIGURE 2.15 Analysis of stresses in a shaft subjected to the combined loads, axial force P and a torque Q .

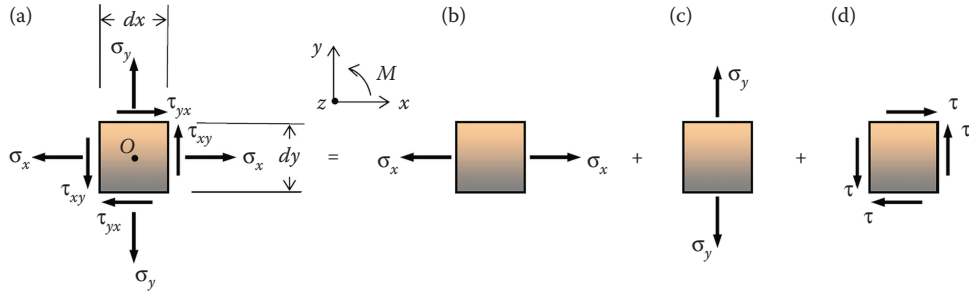


FIGURE 2.16 A general plane-stress condition broken down into three simple components, two uniaxial σ_x and σ_y , and one pure shear τ .

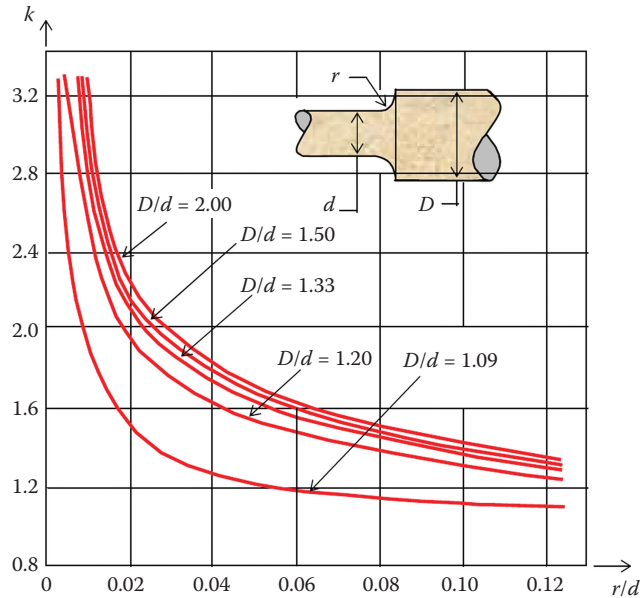


FIGURE 2.17 Stress-concentration factors for torsional loads. (Adapted from the work of L.S. Jacobsen, Torsional stress concentrations in shafts of circular cross section and variable diameter, *Trans ASME*, 47, 619–641, 1925.)

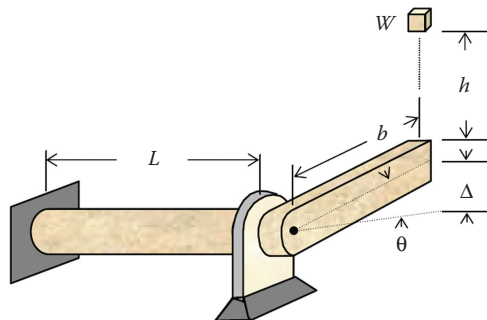


FIGURE 2.18 Diagram showing a shaft of length L subjected to impact loading due to a weight W dropping through a height h .

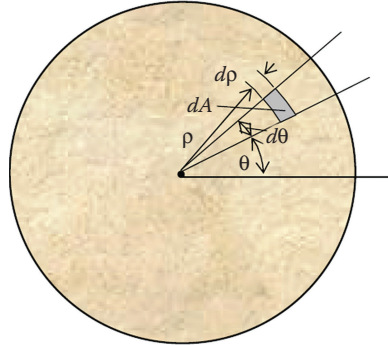


FIGURE 2.20 Cross section of a shaft subjected to a torque T and used to determine the total strain energy U .

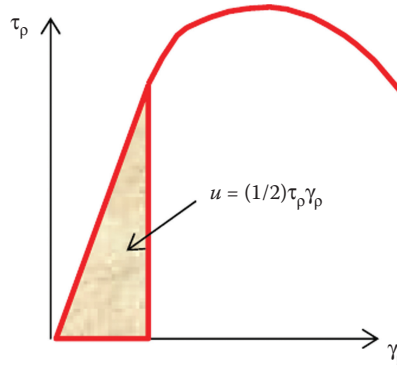


FIGURE 2.19 A shearing stress–strain diagram showing determination of the elastic strain energy u .

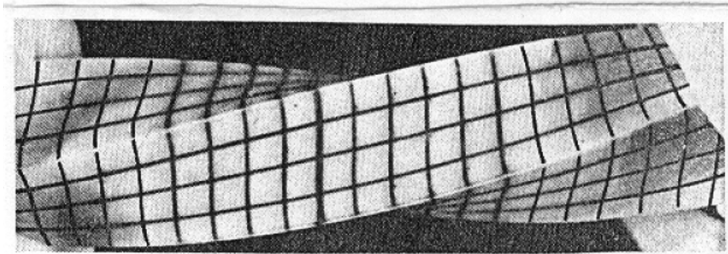


FIGURE 2.22 Diagram showing that, for a shaft of a noncircular cross section, plane sections before twisting do not remain plane after twisting.

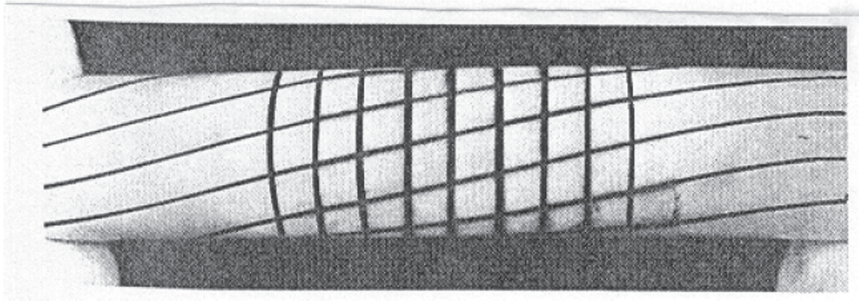


FIGURE 2.21 Diagram showing that, for a shaft of circular cross section, plane sections before twisting remain plane after twisting.

$$\tau_{MAX} = \frac{T(3a + 1.8b)}{8a^2b^2}; \quad \text{occurs at } A$$

$$\theta = \frac{TL}{KG}; \quad K = ab^3 \left[\left(\frac{16}{3} \right) - 3.36 \left(\frac{b}{a} \right) \left(1 - \frac{b^4}{12a^4} \right) \right]$$

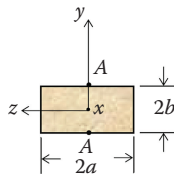


FIGURE 2.24 Mathematically obtained solutions for a shaft of a rectangular cross section.

$$\tau_{MAX} = \frac{2T}{\pi ab^2}; \quad \text{occurs at } A$$

$$\theta = \frac{TL}{KG}; \quad K = \frac{\pi a^3 b^3}{a^2 + b^2}$$

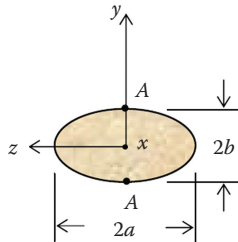


FIGURE 2.23 Mathematically obtained solutions for a shaft of an elliptical cross section.

$$\tau_{MAX} = \frac{20T}{a^3}; \quad \text{occurs at } A$$

$$\theta = \frac{TL}{KG}; \quad K = \frac{(\sqrt{3})a^4}{80}$$

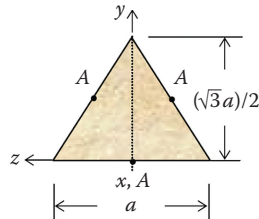


FIGURE 2.25 Mathematically obtained solutions for a shaft of an equilateral triangular cross section.

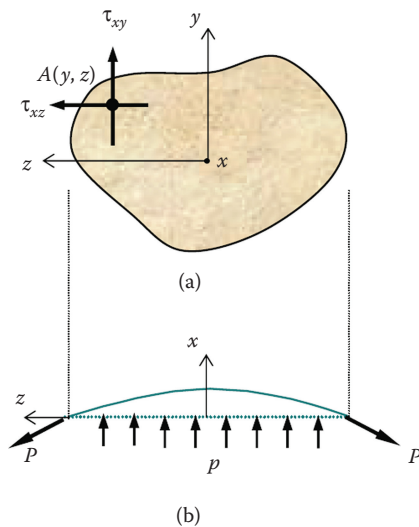


FIGURE 2.26 (a,b) The two views of a distended thin membrane subjected to a pressure p used to experimentally solve the torsion problem of noncircular shafts.

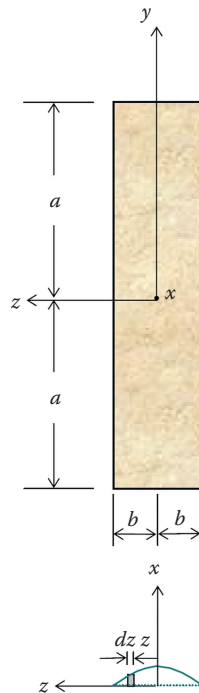


FIGURE 2.27 Experimental solution of the torsion problem of a shaft having a long and thin rectangular cross section.

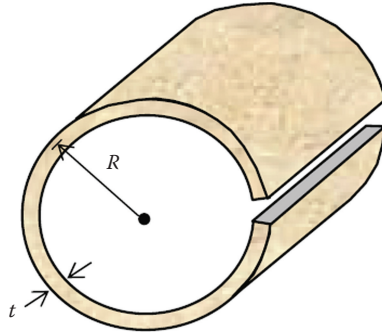


FIGURE 2.28 Solution of the torsion problem of a shaft with a narrow circular section having a thin slit.

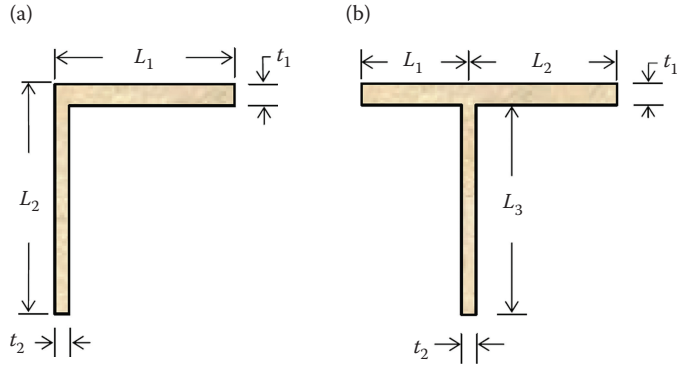


FIGURE 2.29 Diagrams showing cross sections composed of narrow rectangles for which solutions can be obtained.

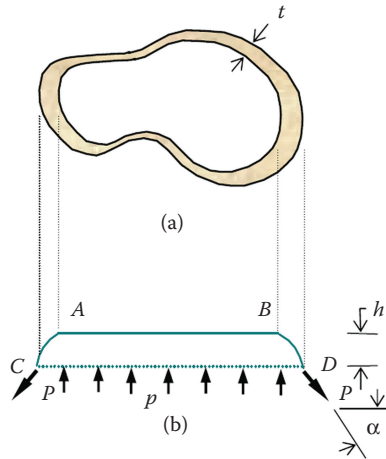


FIGURE 2.30 (a,b) The two views of a distended thin membrane subjected to a pressure p used to experimentally solve the torsion problem of thin-walled tubes of noncircular shafts.

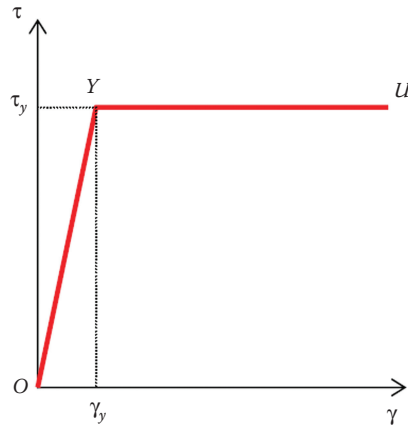


FIGURE 2.31 Stress–strain diagram for an elastoplastic material in which τ_y is the yield stress.

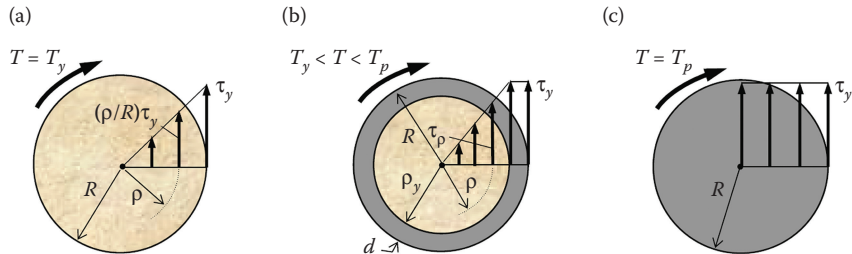


FIGURE 2.32 (a) The shearing stress distribution in a circular shaft when it reaches the yield stress τ_y . (b) The stress distribution when plastic action has reached the outer layers of the circular shaft. (c) The stress distribution when the entire shaft is under plastic action.

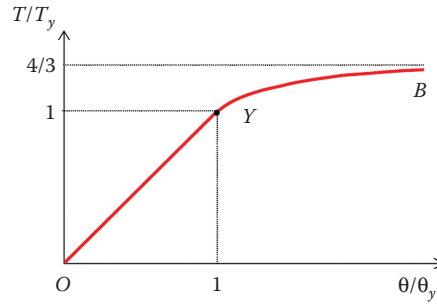


FIGURE 2.33 Diagram showing a plot of Equation 2.65.